Assessment of the Thermodynamic and Fluid Approximations for Electrons in Plasma Thruster Plumes

IEPC-2019-569

Presented at the 36th International Electric Propulsion Conference
University of Vienna, Austria
September 15-20, 2019

Yuan Hu*
Institute of Mechanics, Chinese Academy of Sciences, Beijing, China 100190

Joseph Wang†
University of Southern California, Los Angeles, CA, USA 90089

and

Quanhua Sun‡
Institute of Mechanics, Chinese Academy of Sciences, Beijing, China 100190
University of Chinese Academy of Sciences, Beijing, China 100049

A comparative study on the expansion of a collisionless hypersonic plasma plume into a vacuum in 2D and 3D is presented. The 2D plume is shown to be qualitatively similar to the 3D plume, but quantitative differences exist. The plasma density drops more rapidly in the 3D plume expansion than in the 2D case. The most widely used electron fluid model incoporated into the hybrid PIC is assessed by the fully kinetic data. The hybrid PIC predicts a faster plasma density decrease in both 2D and 3D because of the error introduced by using the electron fluid model. The error is more significant in the 3D case. The inadequacy of the electron fluid model is identified as the strong anisotropic behaviors of electrons. The x-component (plume direction) of electron temperature ($\tilde{T}_{e,x}$) is almost constant and equal to the source temperature inside the plume core region, but shows abnormal enhancement in the outer expansion region. The y-component (radial direction) of electron temperature ($\tilde{T}_{e,y}$) decreases as the plasma expands downstream inside the plume core region, but is elevated outside the plume core as well. However, there are tiny differences in the spatial variations of both $\tilde{T}_{e,x}$ and $\tilde{T}_{e,y}$ inside the plume core between the 2D and 3D plumes. The polytropic coefficient $\gamma_e(\tilde{T}_{e,y} - \tilde{n}_e)$ is smaller in the 3D plume because of its more rapid decrease in the plasma density.

I. Introduction

The expansion of plasma plume from an electric propulsion (EP) thruster is critical for determining the performance of the device and the interaction of the exhaust plasma with spacecraft, e.g. charging, contamination and erosion. As a compromise between accuracy and cost, the hybrid particle-in-cell (PIC) model dominates the previous simulation studies of EP plasma plumes.

One of the most essential issues with accurately applying the hybrid PIC is the closure of the equations governing the electron fluid motions. This is accomplished usually by employing some thermodynamic

*Research Professor, State Key Laboratory of High Temperature Gas Dynamics, yhu@imech.ac.cn.
†Professor, Department of Astronautical Engineering, josephjw@usc.edu.
‡Professor, State Key Laboratory of High Temperature Gas Dynamics, School of Engineering Science, qsun@imech.ac.cn.

relations to close the electron fluid models at the level of momentum equation. The polytropic model relating the isotropic temperature (T_e) to the density (n_e) is often used

$$T_e \propto n_e^{\gamma_e - 1}, \tag{1}$$

where the constant γ_e is the polytropic coefficient. $\gamma_e = 1$ corresponds to the isothermal case, and $\gamma_e = 2$ and 5/3 for the two-dimensional (2D) and three-dimensional (3D) adiabatic process, respectively. To date, the isothermal and adiabatic processes are the most widely used assumptions. Another but more fundamental issue is the validity of the fluid modeling for the electrons. For the fluid model to be applicable, the electrons need to be in local equilibrium. However, the plasma in the EP plume is collisionless, making the equilibrium hard to keep.[1,2]

The fully kinetic method is able to capture the electron kinetics. Due to the huge difference between the electron and ion masses, large scale fully kinetic simulations of collisionless EP plasma plumes with real ion-to-electron mass ratios are extremely expensive, and thereby very rare in the literature. Only recently we have carried out 2D fully kinetic PIC simulations of collisioless plasma plume expansion with the real ion masses of H^+, Ar^+ and Xe^+ for a time scale of $t\omega_{pi} \geq 50$.[3] Our full PIC results find that γ_e is not constant in the plume. Moreover, T_e is highly anisotropic. The electron thermodynamics also depends on the ion masses. Hence, the accuracy of the polytropic electron fluid model needs to be quantitively evaluated by the fully kinetic model.[4–7]

This study extends our recent 2D full PIC simulations to axisymmetric (2D3V) so that 3D effects are included. Compared to the 2D counterparts, the axisymmetric particle simulations are much more expensive because the particle physics is essentially 3D in such simulations. The rest of this paper is organized as follows. Section II describes the simulation model used. Section III presents the simulation results and discussion. Finally, a brief summary and conclusion are given in Section IV.

II. Simulation Model

The simulation setup is shown in Fig. 1. Both fully kinetic and hybrid PIC simulations are carried out. For the fully kinetic PIC simulation, only Xe^+ is considered because it is the the most commonly used propellant of a plasma thruster. The hybrid PIC model used employes the well-known Boltzmann relation, which is derived by assuming the electron is a massless, isothermal ($\gamma_e = 1$) fluid,

$$n_e = n_0 \exp\left[\frac{e(\Phi - \Phi_0)}{k_b T_{e0}}\right], \tag{2}$$

where Φ is the electric potential, k_b is the Boltzmann constant, and the subscript "0" denotes the physical quantities at the reference point. We consider a plasma plume consisting of beam ions and thermal electrons. The temperature ratio of ion to electron at the exit is taken to be $T_{i0}/T_{e0} = 0.01$. The Mach number of the beam ions is set to be $M_0 = v_0/C_{s0} = 20$, where v_0 is the beam velocity and C_{s0} is the ion acoustic speed evaluated according to the beam condition, for all the simulations in this paper. Accordingly, the beam velocity is set to be $v_0/v_{te0} = 0.040734$, where v_{te0} is the electron thermal speed of beam. The ion acoustic speed and electron thermal speed are written as $C_{s0} = \sqrt{k_b T_{e0}/m_i}$ and $v_{te0} = \sqrt{k_b T_{e0}/m_e}$, where m_i and m_e denote the ion and electron masses, respectively. The plume conditions is listed in Table 1. The plume is injected into the simulation domain along the x direction. To simplify the analysis, the beam has a uniform density distribution at the emission surface. The simulation also does not include the small amount of low energy charge-exchange ions generated in the plume of an EP thruster due to computational constrains. As seen in Table 1, the huge gap between the electron and ion characteristic times (ω_{pe0}^{-1} and ω_{pi0}^{-1}), where $\omega_{pe0} = \sqrt{\frac{n_0 e^2}{\epsilon_0 m_e}}$ and $\omega_{pi0} = \sqrt{\frac{n_0 e^2}{\epsilon_0 m_i}}$ are the electron and ion plasma frequencies, respectively, makes fully kinetic PIC simulations with thruster propellents extremely expensive.

Our simulations are performed in the non-dimensional form. The normalization strategies for the fully kinetic and hybrid PIC simulations are different because they need to resolve the plasma dynamics at different time scales. The normalization used for the fully kinetic PIC is as follows,

$$\tilde{m} = \frac{m}{m_e}, \quad \tilde{t} = t\omega_{pe0}, \quad \tilde{\mathbf{v}} = \frac{\mathbf{v}}{v_{te0}}, \quad \tilde{\mathbf{x}} = \frac{\mathbf{x}}{\lambda_{D0}}, \quad \tilde{n} = \frac{n}{n_0}, \quad \tilde{q} = \frac{q}{e}, \quad \tilde{\Phi} = \frac{e\Phi}{k_b T_{e0}}, \tag{3}$$

Table 1. Ion-to-electron mass ratio, plasma plume speed, and electron-to-ion plasma frequency ratio at emission surface

Model	m_i/m_e	v_0/C_{s0}	v_0/v_{te0}	$\omega_{pe0}/\omega_{pi0}$
Hybrid PIC	∞	20	-	-
Full PIC (Xe^+)	241073	20	0.040734	491

and that for the hybrid PIC is,

$$\tilde{m} = \frac{m}{m_i}, \quad \tilde{t} = t\omega_{pi0}, \quad \tilde{\mathbf{v}} = \frac{\mathbf{v}}{C_{s0}}, \quad \tilde{\mathbf{x}} = \frac{\mathbf{x}}{\lambda_{D0}}, \quad \tilde{n} = \frac{n}{n_0}, \quad \tilde{q} = \frac{q}{e}, \quad \tilde{\Phi} = \frac{e\Phi}{k_b T_{e0}}. \tag{4}$$

Both 2D and axi-symmetric simulations are carried out for comparative study. The simulation domain is a rectangular box with $\tilde{L}_x \times \tilde{L}_r = 2000 \times 1000$. The emission source is positioned in the region of $(\tilde{x}, \tilde{y} \,\text{or}\, \tilde{r}) = (0 \sim 6, 0 \sim 20)$. Particles are injected into the simulation domain through the injection plane located at $(\tilde{x}, \tilde{y} \,\text{or}\, \tilde{r}) = (6, 0 \sim 20)$. (We do not distinguish between y and r hereafter.) The electric potential of the source is $\tilde{\Phi}_s = 0$, and a zero-electric field condition is used at the simulation domain boundary. Hence, $\tilde{\Phi}_s$ is floating with respect to the ambient. Any particles (mainly the electrons in the fully kinetic PIC simulations) attracted back to the emission source are removed from the simulation domain. At the boundaries of $\tilde{x} = 0$ and 2000, and $\tilde{y} = 1000$, an absorbing boundary condition for particles is also applied. The simulation is considered to be symmetric with respect to $\tilde{y} = 0$, so the specular reflection condition for the particles and the symmetric condition for the Poisson's solver are imposed at $\tilde{y} = 0$. Because of the symmetric boundary with respect to $\tilde{y} = 0$, the emission source is considered to have a radius of $R_0 = 20\lambda_{D0}$.

The simulation domain is discretized with a uniform mesh. The cell size is $\Delta\tilde{x} = \Delta\tilde{y} = 1$. The time step adopted to push the particles is $\Delta\tilde{t} = \Delta t\omega_{pe0} = 0.05$ in all the full PIC simulations, and $\Delta\tilde{t} = \Delta t\omega_{pi0} = 0.01$ in the hybrid PIC simulation, respectively. The simulations are run sufficiently long ($t\omega_{pi0} \geq 50$) such that the expansion of plasma plume is well developed, but are terminated when the plasma front is still far away from the outflow boundary to minimize the boundary effects on the expansion.

One notable difference between the 2D and axi-symmetric simulations is the distribution of particles. For 2D simulations, the number of particles is distributed uniformly along the transverse or radial (y-) direction if the plasma density keeps the same in that direction. A uniform particle weight is used so the number of macro-particles in a cell scales with the local plasma number density ($\tilde{n}$). For axi-symmetric simulations, the number of particles, instead, increases quadratically along the radial direction as moving away from the center because the volume is proportional to r^2. A consequence of the quadratic increase of particle number in the radial direction is that a relatively larger number of macro-particles has to be used. The reason is if we want to keep the same number of particle per cell in the cells near the axis of symmetry to maintain a low statistical noise, the total number of particles the entire simulation end up with will be large. A remedy for this is to use a non-uniform particle weight so that the number of macro-particles per cell can be maintained almost the same across different r values. A drawback of the non-uniform particle weight scheme is that the split or merge of macro-particles when they cross cells will introduce additional errors, even with the state-of-art strategies.[8,9] Typically, over 160 and 360 million macro-particles are tracked at the end of the

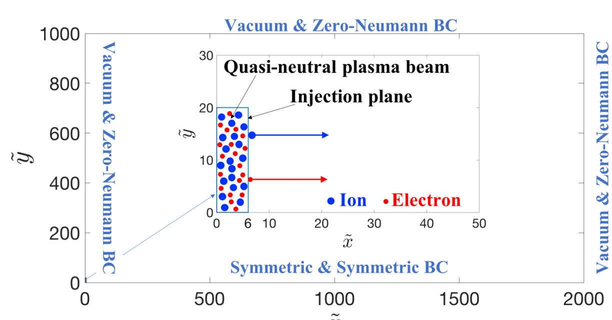

Figure 1. Schematics of the simulation setup for a collisionless hypersonic plume expansion into a vacuum.

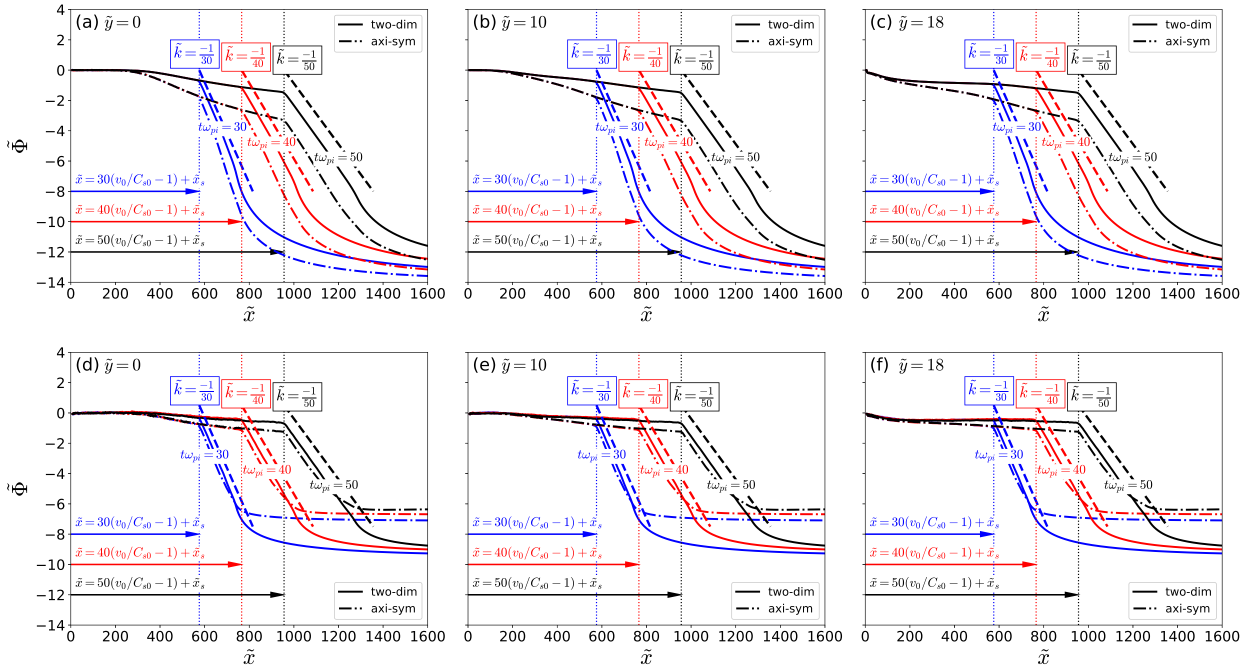

Figure 2. One-dimensional electric potential profiles along the x-axis (plume direction) inside the core region for $t\omega_{pi}$ = 30 (blue), 40 (red) and 50 (black). The upper (a, b, c) and lower (d, e, f) panles show the results from the hybrid PIC and full PIC simulations, respectively. The profiles are extracted along $\tilde{y}$ = (a, d) 0, (b, e) 10, and (c, f) 18.

2D and axi-symmetric plume simulations, respectively.

III. Results and Discussions

A. Evolution of plasma plume

The simulation results up to $t\omega_{pi} = 50$ are presented. Longer simulations (up to $t\omega_{pi0} = 60$) were run, but not shown, to ensure the conclusions are still valid at later time.

Fig. 2 shows the time evolution of the 1D electric potential profiles along the x-axis (plume direction) inside the core plume region at $t\omega_{pi} = 30$, 40 and 50. The comparisons between the 2D and axi-symmetric plumes from both hybrid and full PIC simulations are presented. The most remarkable observation is that the axi-symmetric plume has the same four distinct plasma regions as the 2D plume, which is first discussed in detail in Ref.,[3] and exhibits the same evolution trend.

The first region is the unperturbed region (1). In this region, the electric potential is almost constant for both 2D and axi-symmetric plumes. Followed by the unperturbed region is the quasi-steady expansion region (2), where the potential decreases along the plume direction with a moderate rate. The boundary between the quasi-steady region (2) and the self-similar expansion region (3) propagates downstream with a constant speed. It is surprising to see that propagation speed of the boundary between region (2) and (3) for the axi-symmetric plume is also $v_0 - C_{s0}$, the same as that for the 2D plume. The comparison between the 2D and axi-symmetric plumes in the quasi-steady expansion region shows that the potential in the axi-symmetric plume drops with a faster rate. The faster potential decrease in the axi-symmetric plume is signified by the hybrid PIC modeling. The 2D and axi-symmetric plume have almost the identical pattern of the self-similar expansion region. The slope of the potential drop in the this region is well described by the theory based on the 1D semi-infinite plasma model. Though the self-similar expansion characteristics is the same for both 2D and axi-symmetric plumes, the self-similar expansion region ends or the pure electron region (4) appears much earlier in the latter one. A consequence of this is that the axi-symmetric case has a smaller total potential drop across the entire domain compared with the 2D plume.

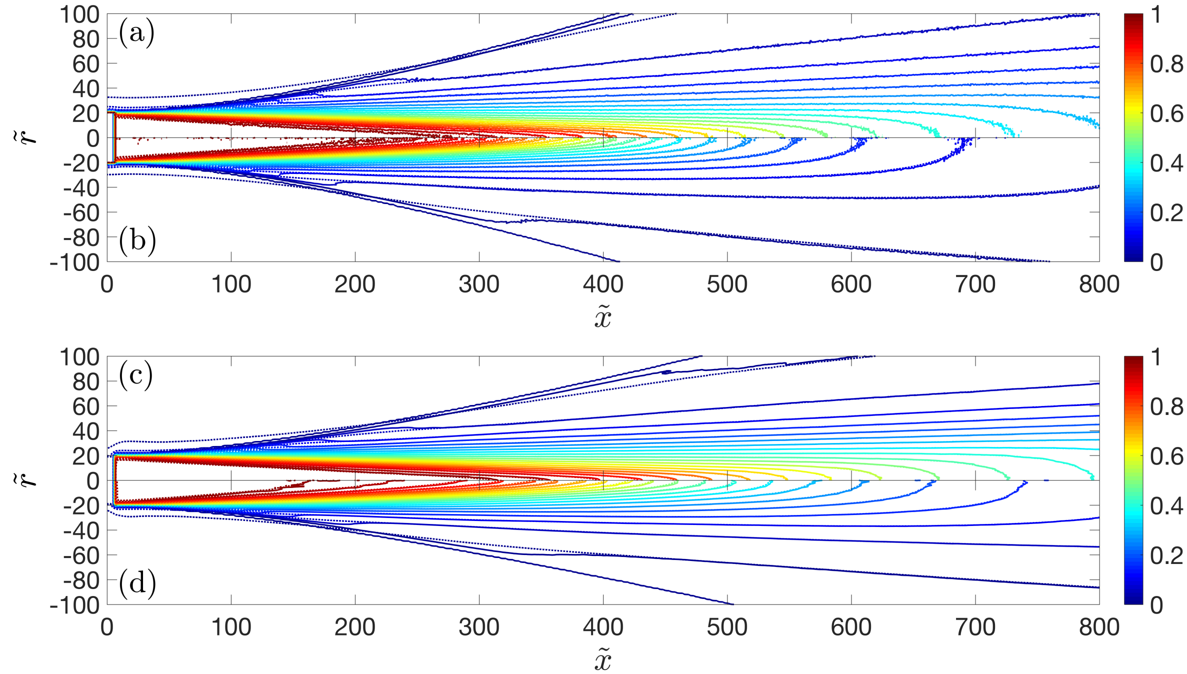

Figure 3. (Color) Iso-contour lines of the ion ("———") and electron ("– – –") number density at the steady state: (a) two-dimensional hybrid PIC, (b) axi-symmetric hybrid PIC, (c) two-dimensional full PIC and (d) axi-symmetric full PIC.

B. Steady state plasma plume

In real EP applications, people may be more interested in the steady state operation not far away from the thruster. The plume evolution shown in Fig. 2 has provided us with solid evidence about when and where the plume reaches a steady state. For instance, the region with $\tilde{x} \leq 800$ is guaranteed to reach a steady state after $t\omega_{pi} \geq 50$.

Fig. 3 and Fig. 4 show the steady state ($t\omega_{pi} = 50$) iso-density lines and 1D profiles along plume direction, respectively. The 2D and axi-symmetric plume structures from both hybrid and fully kinetic PIC simulations are compared. It is clear that, in the steady state region, the plume is quasi-neutral, namely $\tilde{n}_i \simeq \tilde{n}_e$. The pattern of the 2D plasma plume agrees qualitatively with the axi-symmetric plasma plume, despite that the density in the 2D plasma decreases with a slower rate outside the unperturbed region. Such quantitative difference between the 2D and axi-symmetric plumes is more significant in the hybrid PIC modeling than in the fully kinetic PIC modeling. The difference in the density profiles is also consistent with the observation on the potential profiles shown in Fig. 2.

Fig. 5 compares the ion streamlines for different models. The ion streamlines start from the plasma injection plane. Three different positions, $\tilde{y} = 2$, 10, and 18, along the injection plane are shown in Fig. 5. In general, the ion trajectories are deflected more when the origin is further away from the center of the plume. The hybrid PIC simulations predict much larger divergence angle for the ion streamlines than the full PIC simulations. In terms of the 3D effects, the ions are deflected more in the axi-symmetric plumes. A larger divergence is expected in the axi-symmetric plume because the density drop is more rapid and the mass should be conserved.

The steady state electron temperature contours are shown in Fig. 6. The ion streamlines starting from several representative locations are also overlaid. $\tilde{T}_{e,x}$ is observed to maintain the source temperature inside the core plume region ($\tilde{y} \lesssim \tilde{R}_0$) as the plume propagates downstream, for not only the 2D but also the axi-symmetric case. This also explains why the boundary between region (2) and (3) propagates with a constant speed $v_0 - C_{s0}$, which requires an isothermal condition to be valid, seen in Fig. 2. $\tilde{T}_{e,y}$ inside the plume core region is observed to decrease quickly as the plasma propagates downstream. Fig. 7 shows a comparison of the 1D electron temperature profiles extracted along the plume direction inside the core region between the 2D and axi-symmetric cases. It is surprising to see a negligible difference in the electron temperature profiles

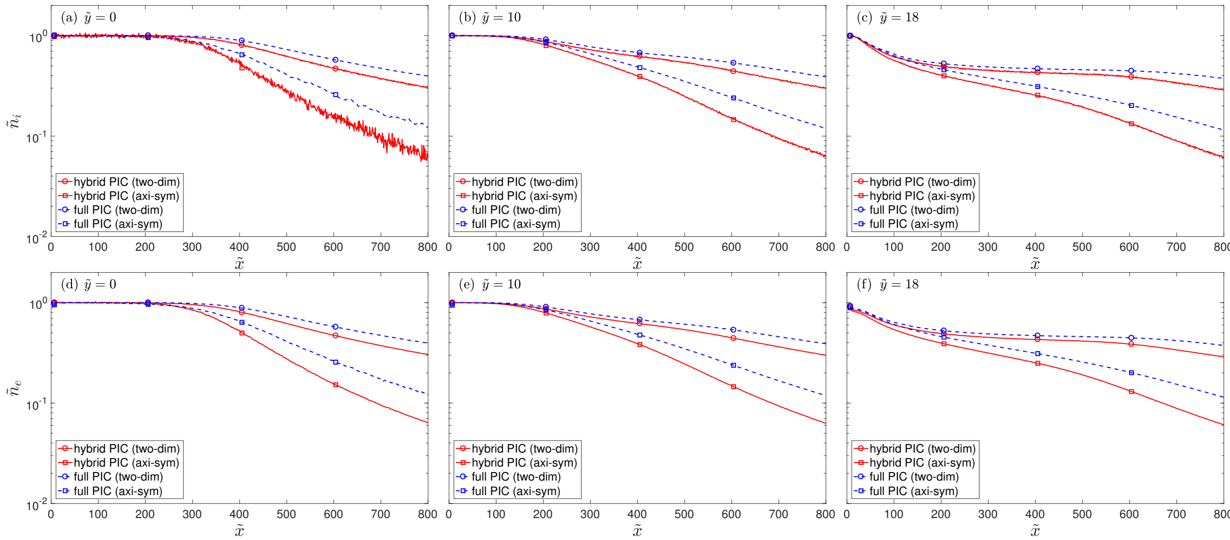

Figure 4. One-dimensional plasma density profiles along the x-axis (plume direction) inside the core region for the steady state results, a comparison between the two-dimensional and axi-symmetric results from both hybrid and full PIC simulations. The upper (a, b, c) and lower (d, e, f) panles show the ion and electron densities, respectively. The profiles are extracted along $\tilde{y}$ = (a, d) 0, (b, e) 10, and (c, f) 18.

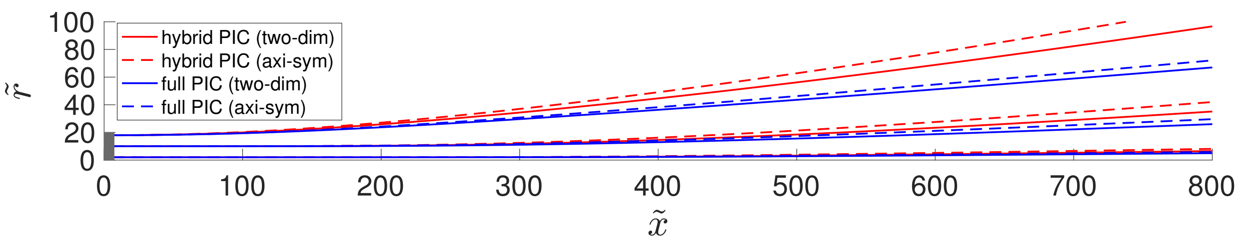

0

Figure 5. Ion streamlines starting from the injection plane $\tilde{x} = 6$ for $\tilde{y}$ = 2, 10, and 18, a comparison between the two-dimensional and axi-symmetric results from both hybrid and full PIC simulations.

inside the plume core region between the 2D and axi-symmetric cases.

The electron temperatures outside the plume core region exhibits some abnormal characteristics. Instead of cooling, the temperature of electron may undergo an increase in the expansion region as its density decreases. In particular, both $\tilde{T}_{e,x}$ and $\tilde{T}_{e,y}$ are considerably enhanced in the region outside the outermost ion streamline. The abnormal electron temperature enhancement is mainly due to the kinetic behaviors of the electrons in the low density region, similar to what has been discussed in the plasma wake of plate discussed in Refs.[10,11]

C. Electron thermodynamics

The comparison between the hybrid and full PIC results have provided sound evidence that the electron fluid appproximation is inadequate for studying the expansion of a collisionless plasma plume into a vacuum, especially in the region outside the plume core region where the electron kinetic effects are important and abnormal electron thermodynamic properties are seen. However, the fully kinetic approaches, though very accurate, are much more computationlly expensive than the fluid based methods. As a result, the fluid based modelings of the plasma plume expansion, including full fluid and hybrid fluid-kinetic methods, are still heavily used. A popular method is to employ the polytropic law, Eq. 1, to describe the electron thermodynamics mainly due to its simplicity but better generalizability than the isothermal assumption. The proper choice of the polytropic coefficient γ_e is the key for accurate modelings. However, lacking reliable high fildelity data, the selection of γ_e is somewhat arbitary in practice.[5,7,12]

Fig. 8 shows the $\log_{10}\tilde{T}_e - \log_{10}\tilde{n}_e$ relation along several representative ion streamlines for both 2D and axi-symmetric plumes in the steady state region. Note that the polytropic coefficient can be obtained from

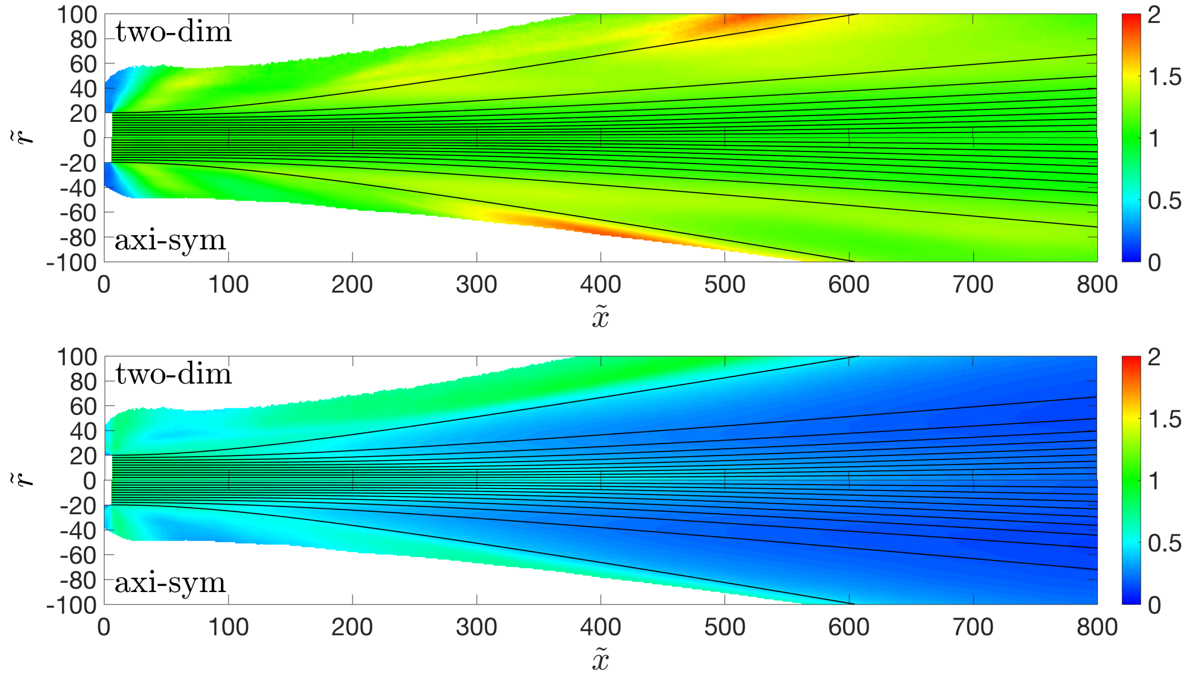

Figure 6. (Color) Iso-contour lines of the ion ("———") and electron ("– – –") number density at the steady state: (a) two-dimensional hybrid PIC, (b) axi-symmetric hybrid PIC, (c) two-dimensional full PIC and (d) axi-symmetric full PIC.

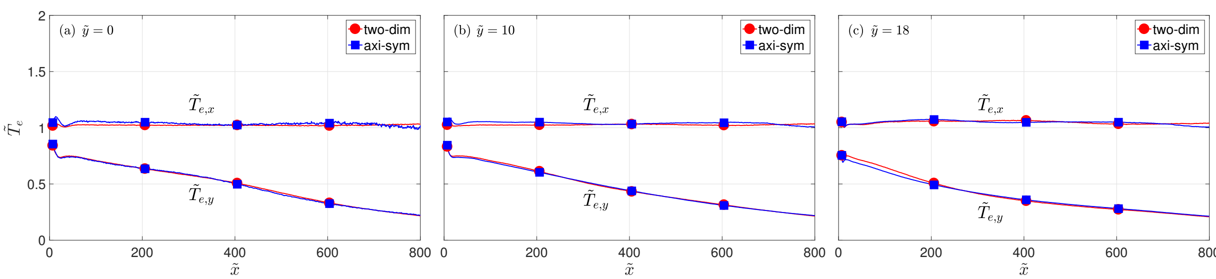

Figure 7. One-dimensional electron temperature profiles along the x-axis (plume direction) inside the core region for the steady state full PIC results, a comparison between the two-dimensional and axi-symmetric results. The profiles are extracted along $\tilde{y}$ = (a) 0, (b) 10, and (c) 18.

the slopes (k) of the lines on the $\log_{10}\tilde{T}_e - \log_{10}\tilde{n}_e$ plot, that is $\gamma_e = \delta\gamma_e + 1 = k + 1$. The polytropic relations are plotted along the ion streamlines because we consider the ion dynamics is the only concern in a fluid bases modeling. First of all, the strong anisotropic themodynamic properties of electrons are clearly seen for both 2D and axi-symmetric plumes. Along the ion streamline whose origin $\tilde{y}$ is within 12, $\delta\gamma_e(\tilde{T}_{e,x} - \tilde{n}_e)$ is approximately 0, indicating isothermal processes. The $\log_{10}\tilde{T}_{e,y} - \log_{10}\tilde{n}_e$ plots show almost linear relations along the same set of ion streamlines for both 2D and axi-symmetric cases. The data is fitted to a linear relation to get the slope (k) of each set of $\log_{10}\tilde{T}_{e,y} - \log_{10}\tilde{n}_e$, and thus the polytropic coefficient $\gamma_e(\tilde{T}_{e,y} - \tilde{n}_e)$. It is found that $\gamma_e(\tilde{T}_{e,y} - \tilde{n}_e)$ slightly increases as the origin of the ion streamline moves away from the center. Overall, $\gamma_e(\tilde{T}_{e,y} - \tilde{n}_e) \simeq 2.1$ and 1.6 for the 2D and axi-symmetric plumes, respectively. It is noted that, for a monotonic gas like electron, $\gamma_e = 2$ and $5/3$ for the 2D and 3D adiabatic processes, respectively. $\gamma_e(\tilde{T}_{e,y} - \tilde{n}_e)$ obtained in the present full PIC simulations is close to the values for adiabatic processes when the ion streamlines are close to the plume center. However, it should be emphasized that this does not mean the expansion process is an adiabatic, or even a hydrodynamic process due to the strong anisotropic electron kinetics. In addition, for the ion streamlines which are closer to the edge of the plasma source ($\tilde{y} \geq 14$), the simple polytropic relation completely fails to describe the electron thermodynamics, as

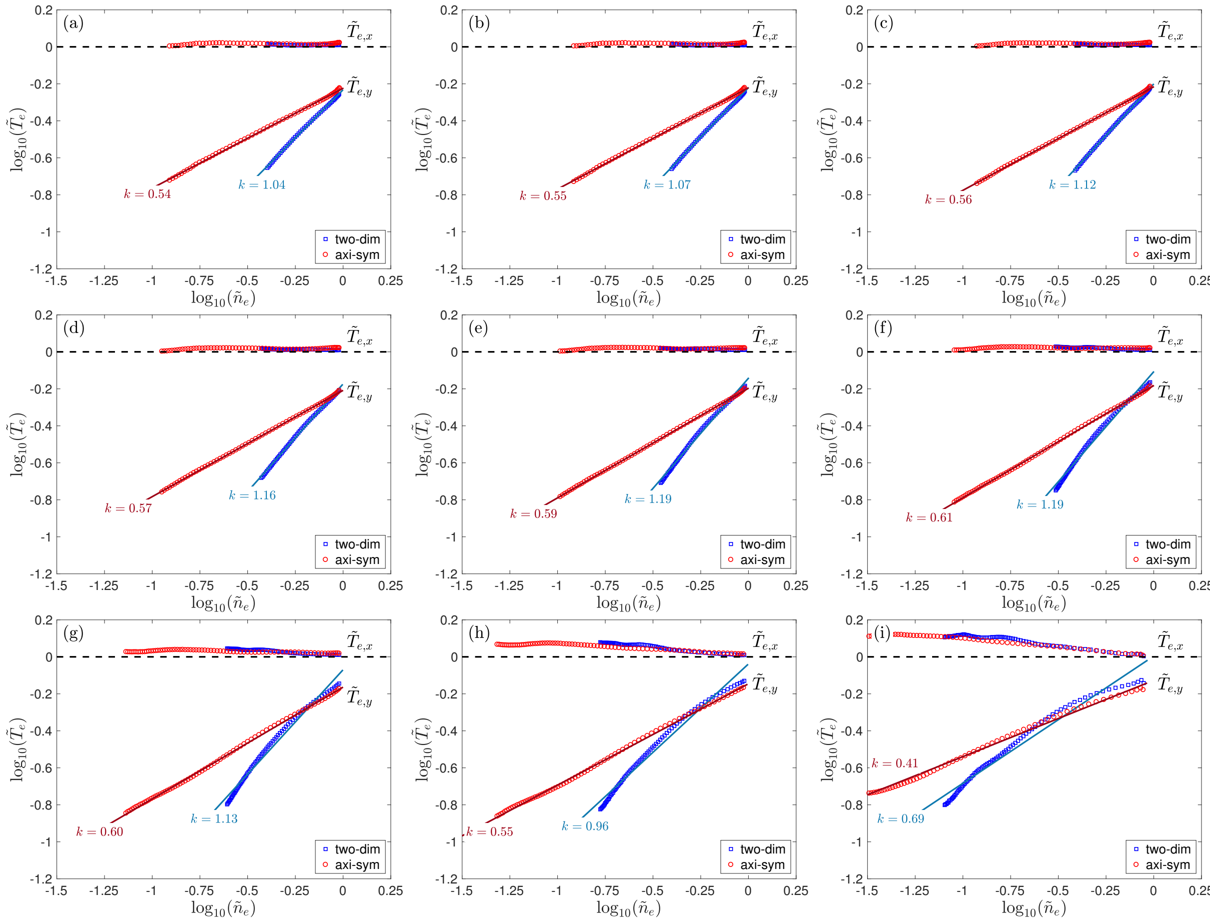

Figure 8. $\log_{10}(\tilde{T}_e) - \log_{10}(\tilde{n}_e)$ **along the ion streamlines starting from the injection plane** $\tilde{x} = 6$ **at various** $\tilde{y}$ **positions: (a) 2, (b) 4, (c) 6, (d) 8, (e) 10, (f) 12, (g) 14, (h) 16, and (i) 18.**

shown in Figs. 8 (g)∼(i).

IV. Summary and Conclusion

This paper presents a comparative study of the expansion of a collisionless hypersonic plasma plume into a vacuum in 2D and 3D. Both hybrid and fully kinetic PIC simulations are carried out. The comparison shows that the 2D plume is qualitatively similar to the 3D plume, but quantitative differences exist. The plasma density drops more rapidly in the 3D plume expansion than in the 2D plume. The more rapid decrease in the plasma density profile in the 3D plume is signified by the hybrid PIC modeling. The electrons exhibit strong anisotropic behaviors in both 2D and 3D plume expansions. $\tilde{T}_{e,x}$ is almost constant and equal to the source temperature inside the plume core region, but shows abnormal enhancement in the outer expansion region. $\tilde{T}_{e,y}$ decreases as the plasma expands downstream inside the plume core region, but is elevated unusually in the outside region as well. The differences in the spatial variations of electron temperatures between the 2D and 3D plumes are very small inside the plume core region. As a result, the smaller $\gamma_e(\tilde{T}_{e,y} - \tilde{n}_e)$ for the 3D plume is due to the more rapid decrease of the plasma density. The fully kinetic PIC results show that the fluid models are generally inadequate for the collisionless plasma plume expansion because the electron kinetic behaviors are mainly non-equilibrium, especially in the outer expansion region.

References

[1]Othmer, C., Glassmeier, K., Motschmann, U., Schüle, J., and Frick, C., "Three-Dimensional Simulations of Ion Thruster Beam Neutralization," *Physics of Plasmas*, Vol. 7, No. 12, 2000, pp. 5242–5251.

[2]Hu, Y. and Wang, J., "Fully kinetic simulations of collisionless, mesothermal plasma emission: Macroscopic plume structure and microscopic electron characteristics," *Physics of Plasmas*, Vol. 24, No. 3, 2017, pp. 033510.

[3]Hu, Y. and Wang, J., "Expansion of a collisionless hypersonic plasma plume into a vacuum," *Physical Review E*, Vol. 98, No. 2, 2018, pp. 023204.

[4]Denavit, J., "Collisionless Plasma Expansion into a Vacuum," *Phys. Fluids*, Vol. 22, No. 7, 1979, pp. 1384–1392.

[5]Merino, M. and Ahedo, E., "Influence of electron and ion thermodynamics on the magnetic nozzle plasma expansion," *IEEE Transactions on Plasma Science*, Vol. 43, No. 1, 2015, pp. 244–251.

[6]Hu, Y. and Wang, J., "Electron properties in collisionless mesothermal plasma expansion: Fully kinetic simulations," *IEEE Transactions on Plasma Science*, Vol. 43, No. 9, 2015, pp. 2832–2838.

[7]Cichocki, F., Domínguez-Vázquez, A., Merino, M., and Ahedo, E., "Hybrid 3D model for the interaction of plasma thruster plumes with nearby objects," *Plasma Sources Science and Technology*, Vol. 26, No. 12, 2017, pp. 125008.

[8]Pfeiffer, M., Mirza, A., Munz, C.-D., and Fasoulas, S., "Two statistical particle split and merge methods for Particle-in-Cell codes," *Computer Physics Communications*, Vol. 191, 2015, pp. 9–24.

[9]Vranic, M., Grismayer, T., Martins, J. L., Fonseca, R. A., and Silva, L. O., "Particle merging algorithm for PIC codes," *Computer Physics Communications*, Vol. 191, 2015, pp. 65–73.

[10]Wang, J. and Hu, Y., "The breakdown of the fluid approximation for electrons in a plasma wake," *J. Geophys. Res. Space Phys.*, Vol. 123, 2018, pp. 8797–8805.

[11]Hu, Y. and Wang, J., "Assessment of electron thermodynamics and fluid approximations for collisionless plasma expansion into a wake," *Phys. Plasmas*, Vol. 26, 2019, pp. 023515.

[12]Merino, M., Cichocki, F., and Ahedo, E., "A Collisionless Plasma Thruster Plume expansion Model," *Plasma Sources Sci. Technol.*, Vol. 24, No. 3, 2015, pp. 035006.